

Global optimization and structural analysis of Coulomb and logarithmic potentials on the unit sphere using a population-based heuristic approach

Xiangjing Lai^a, Jin-Kao Hao^{b,*}, Renbin Xiao^c and Zhang-Hua Fu^d

^a*Institute of Advanced Technology, Nanjing University of Posts and Telecommunications, Nanjing, 210023, China*

^b*LERIA, University of Angers, 2 Boulevard Lavoisier, Angers, 49045, France*

^c*School of Artificial Intelligence and Automation, Huazhong University of Science and Technology, Wuhan, 430074, China*

^d*Institute of Robotics and Intelligent Manufacturing, The Chinese University of Hong Kong, Shenzhen, 518172, China*
Expert Systems with Applications 238 (Part A) 121704 March 2024

ARTICLE INFO

Keywords:

Gradient-based optimization
Minimum energy configuration
Discrete logarithmic potential
Thomson problem
Global optimization

Abstract

Global optimization of high-dimensional non-convex functions arises in many important applications and researches. In this paper, we focus on the minimum energy configuration problem on the unit sphere, whose goal is to determine the minimum-energy configuration of N particles interacting via the standard Coulomb potential or the discrete logarithmic potential on the unit sphere. This is a classic global optimization problem with many important applications in mathematics, physics, biology and chemistry, and is one of the 18 great mathematical problems for the twenty-first century listed by the Fields Medal winner S. Smale (Smale, 1998). To determine the minimum-energy configuration for these two potential functions, we propose a population-based global optimization algorithm that combines a two-phase local optimization method with early-stopping strategy, a random perturbation operator, a distance-based population update strategy using a novel distance function to measure the difference between solutions, and a population rebuilding method. Computational results show that the proposed algorithm is very competitive compared to the best known results in the literature. In particular, it improves the best-known result for one instance of the classic Thomson problem (i.e., $N = 360$) widely studied in the literature. The configurations of instances with up to $N = 500$ particles are systematically optimized for the first time by the proposed algorithm for the discrete logarithmic potential. The comparative study shows that the putative optimal configurations have a high similarity for the Coulomb and logarithmic potentials and that the defects play an important role in reducing the energy of configuration. The energies of particles on the putative optimal configurations are analyzed for the studied logarithmic potential.

1. Introduction

Global optimization of high-dimensional non-convex functions with a first-order derivative arises in a number of researches and applications, such as the predictions of ground-state structures of clusters, crystals, and biomolecules (Wei, 2019; Doye, Leary, Locatelli and Schoen, 2004; Wales and Scheraga, 1999; Wales and Ulker, 2006). In general, global optimization is computationally challenging due to the fact that the number of local minima on the potential energy surface (PES) of the objective function increases exponentially as the problem size increases, the highly competing local minima may be separated from each other by high barriers on the PES (Doye, Miller and Wales, 1999), while the global optimum solution may locate at a very narrow and deep funnel on the PES of objective function. A large number of studies have been dedicated to global optimization problems, such as those reported in (Shao, Shangguan, Tao, Zheng, Liu and Wen, 2018; She, Fournier, Yao, Wang and Hu, 2022; Dao, Abhary and Marian, 2017; Leary, 2000; McAllister and Floudas, 2010; Wales and Scheraga, 1999). In this paper, we focus on the minimum energy configuration problem on the unit sphere (Calkin, Kiang and Tindall, 1986; Smale, 1998), which is

*Corresponding author.

*Jin-Kao Hao

 laixiangjing@gmail.com (X. Lai); jin-kao.hao@univ-angers.fr (J. Hao); rbxiao@hust.edu.cn (R. Xiao); fuzhanghua@cuhk.edu.cn (Z. Fu)

ORCID(s): 0000-0002-1101-3056 (X. Lai); 0000-0001-8813-4377 (J. Hao); 0000-0003-0951-2734 (R. Xiao); 0000-0002-3740-7408 (Z. Fu)

a classical global optimization problem with a number of important applications in e.g. mathematics, physics, biology and chemistry.

Given N identical particles $\omega_N = \{r_1, r_2, \dots, r_N\}$ interacting via a pairwise potential $E(\omega_N)$ on the surface of the unit sphere $S^2 = \{r \in R^3 : \|r\| = 1\}$, the minimum energy configuration problem on the unit sphere is to determine the lowest-energy configuration of these N particles. In mathematics and physics, one of the most widely-studied potentials is the Riesz s -energy (Saff and Kuijlaars, 1997). Specifically, given N identically charged particles $\omega_N = \{r_1, r_2, \dots, r_N\}$ confined on the unit sphere S^2 and a positive real-valued number s ($s > 0$), the Riesz s -energy $E_s(\omega_N)$ of ω_N is defined as (Hardin and Saff, 2005):

$$E_s(\omega_N) = \sum_{i=1}^{N-1} \sum_{j=i+1}^N \frac{1}{\|r_i - r_j\|^s}. \quad (1)$$

where $\|r_i - r_j\| = \sqrt{(x_i - x_j)^2 + (y_i - y_j)^2 + (z_i - z_j)^2}$, (x_i, y_i, z_i) and (x_j, y_j, z_j) denote respectively the Cartesian coordinates of the particles r_i and r_j .

When $s = 1$, the Riesz s -energy is the well-known Coulombic potential, and the corresponding global optimization problem is called the Thomson problem which was originally proposed by J.J. Thomson in 1904 (Thomson, 1904).

When s approaches to 0, the potential function takes another formulation that is called the discrete logarithmic potential and can be written as follows (Dragnev, Legg and Townsend, 2002):

$$E_0(\omega_N) = \sum_{i=1}^{N-1} \sum_{j=i+1}^N \log\left(\frac{1}{\|r_i - r_j\|}\right) \quad (2)$$

It is worth noting that the minimization of the potential function $E_0(\omega_N)$ is equivalent to the maximization of the product of distances between particles (i.e., $\prod_{i < j} \|r_i - r_j\|$) (Smale, 1998).

Determining the minimum energy configuration of N particles interacting via the Coulombic potential or the discrete logarithmic potential on the unit sphere is a very difficult task. This is especially true when large instances with $N \geq 400$ are considered. This is because the number of local optimal solutions increases exponentially with the number (N) of particles (Erber and Hockney, 1995), and the computational complexity of locating a local minimum solution grows quadratically with N and thus the local optimizations are very time-consuming even for the medium instances. Thus, these problems are usually used as benchmark systems for evaluating the performance of various global optimization algorithms in the literature. Moreover, together with several other well-known mathematical problems like the Riemann Hypothesis, Poincaré conjecture and the computational complexity problem “Does P = NP?”, the minimum energy configuration problems on the unit sphere with the Coulombic and the discrete logarithmic potentials are among the 18 great mathematical problems for the twenty-first century listed by the Fields Medal winner S. Smale (Smale, 1998).

The minimum energy configuration problems on the sphere with the Coulombic potential and the discrete logarithmic potential have numerous applications in various fields. For example, the global minimum solutions of the Thomson problem (with the Coulombic potential) are typically related to the ground-state structures of spherical viruses (Baker, Olson and Fuller, 1999; Li, Roy, Travesset and Zandi, 2018; Martín-Bravo, Llorente, Hernández-Rojas and Wales, 2021; Zandi, Dragnea, Travesset and Podgornik, 2020), so determining the global minimum solution of the Thomson problem can help to determine the geometrical structures of many spherical viruses. A number of molecules have a spherical structure (e.g., C_{60} molecules), which corresponds to the global minimum solution of the corresponding Thomson problem (Kroto, Heath, O’Brien, Curl and Smalley, 1985; Wales, McKay and Altschuler, 2009; Saff and Kuijlaars, 1997), where the atoms are arranged on a spherical surface. In electrostatics, locating identical point charges on a sphere so that the Coulomb potential of the system is minimized is an important and challenging problem (Bowick, Cacciuto, Nelson and Travesset, 2002; Saff and Kuijlaars, 1997). In addition, determining the global minimum solution of the logarithmic potential on the sphere is a relevant issue in the field of computational complexity (Smale, 1998; Saff and Kuijlaars, 1997).

Due to the practical importance and computational difficulty of the minimum energy configuration problems on the sphere, a large number of theoretical and computational studies have been reported in the literature to predict and describe the global minimum solutions. Indeed, research on more efficient algorithms able to better solve these problems will significantly contribute to finding better solutions to many practical problems as well. In this work, we

focus on computational methods and provide the following related literature review. For the related theoretical studies, the interested readers are referred to (Katanforoush and Shahshahani, 2003; Saff and Kuijlaars, 1997).

In 1986, Wille proposed a simulated annealing algorithm for the Thomson problem and reported the first putative optimal configurations for $N \leq 20$ (Wille, 1986). In 1994, Altschuler et al. presented a Monte Carlo algorithm based on the Metropolis accepting criterion and reported the putative optimal solutions for $66 \leq N \leq 100$. In 1995, Erber and Hockney further improved the best-known results for $N = 69, 86, 87$. In 1996, Morris et al. introduced a genetic algorithm and reported the putative optimal solutions for $N \leq 200$ (Morris, Deaven and Ho, 1996).

In 1997, Altschuler et al. studied the possible global minimum lattice configurations for the Thomson problem (Altschuler, Williams, Ratner, Tipton, Stong, Dowla and Wooten, 1997) and conjectured that the icosahedral lattice configurations are the global minimum solutions for $N = 10(p^2 + q^2 + pq) + 2$ where p and q are positive integers. However, by improving the best-known results for some large instances, Pérez-Garrido et al. subsequently pointed out that the icosahedral lattice configurations are not necessarily the global minimum configurations for these N values. To systematically analyze the global minimum structures of the Thomson problem, in 2006 and 2009 (Wales and Ulker, 2006; Wales et al., 2009), Wales et al. predicted the global minima for a number of instances by the popular basin hopping algorithm (Wales and Doye, 1997). Their computational results further confirmed that the icosahedral lattice configurations are not necessarily the global minimum configurations especially for large instances and that adding dislocation defects to icosahedral lattice configurations is able to efficiently lower their energies.

In 2015, Calef et al. investigated the number of local minima for the generalized Thomson problem (Calef, Griffiths and Schulz, 2015) and confirmed that the number of local minima grows exponentially with the number N of particles. At the same year, Mehta et al. explored the potential energy landscape of the Thomson problem via the Newton homotopies method (Mehta, Chen, Morgan and Wales, 2015). In 2016, Mehta et al. further showed that the local minima are always close to the global minimum solution for small instances with $N \leq 147$, and that the set of local minima exhibits a small-world network (Mehta, Chen, Chen, Kusumaatmaja and Wales, 2016). In 2018, Ridgway and Cheviakov proposed an iterative optimization method for locating the global minimum solution for four potential functions, including the Coulombic and discrete logarithmic potentials, and reported the putative global minimum for small instances with $N \leq 65$ for these potentials (Ridgway and Cheviakov, 2018).

As demonstrated above, the minimum energy configuration problem studied in this work is an important mathematical problem as well as a very representative global optimization problem. However, due to their high computational complexity, most of existing computational studies focus on small instances (with $N \leq 200$), and there are few computational studies for solving large instances especially for the discrete logarithmic potential. The present study aims to fill this gap by proposing an efficient global optimization algorithm for dealing with large instances for both the Coulombic and the discrete logarithmic potentials and making a meaningful analysis for the putative optimal configurations found by the algorithm.

The main contributions of this work are summarized as follows. First, we propose a global optimization algorithm for the minimum energy configuration problems on the unit sphere with the Coulombic and the discrete logarithmic potentials, which can be viewed a new variant of the popular population-based basin-hopping (PBH) algorithm (Grosso, Locatelli and Schoen, 2007). The algorithm combines a two-phase local optimization using an early-stopping technique and a specific perturbation operator and is reinforced by a distance-based population updating strategy and a population rebuilding method. Second, we report the putative optimal configurations with up to $N = 500$ particles for the discrete logarithmic potential and analyze the structural evolution and feature of these configurations as the number of particles increases. Third, due to its general nature, the proposed algorithm can be applied to solve other global optimization problems, including, in particular, the general Riesz s -energy. Finally, since the studied minimum energy problems have a number of relevant applications in diverse fields, the proposed algorithm can contribute to research in these applied fields, and the program codes of the proposed algorithm that we make publicly available will facilitate such applications.

The rest of paper is organized as follows. Section 2 describes the proposed algorithm in detail. In Section 3, the algorithm is evaluated based on a number of popular benchmark instances. In Section 5, we analyze two key algorithmic components and shed light on their impacts on the performance of the algorithm. Section 4 investigates the structural evolution and features of putative optimal configurations for the discrete logarithmic potential, makes a comparative study between the Coulomb potential and the discrete logarithmic potential on the putative optimal configurations, and analyzes the energy distribution of particles of the putative optimal configurations for the logarithmic potential. Finally, we summarize the present work and provide research perspectives in the last section.

2. Global Optimization Method

Evolutionary algorithms with gradient-based local optimization are shown to be very efficient for global optimization problems with a differentiable objective function and a large number of local minima, such as those in (Gudla and Ganguli, 2005; Shang, Zhang and Yang, 2021; Vitela and Castaños, 2012; Wales and Scheraga, 1999), where the most representative example is the population-based basin-hopping (PBH) algorithm (Grosso et al., 2007) that has been applied to a number of global optimization problems in the literature, such as the circle packing problem (Grosso, Jamali, Locatelli and Schoen, 2010), the molecular distance geometry problems (Grosso, Locatelli and Schoen, 2009), and the structural optimization of atomic clusters (Grosso et al., 2007). In this section, we present a global optimization algorithm called the hybrid evolutionary algorithm (HEA), which can be seen as a strengthened variant of the PBH algorithm (Grosso et al., 2007), for the minimum energy configuration problem on the unit sphere with the Coulombic and discrete logarithmic potentials. The algorithm combines a gradient-based local optimization method and the population-based evolutionary search framework. We first introduce the general approach of transforming the initial constrained problems into an unconstrained problem and then explain how the transformed problem is solved by the proposed algorithm.

2.1. Unconstrained formulation of constrained optimization problems

Global optimization of a system with N particles is a hot research topic in physics, chemistry and biology, such as the structural optimization of atomic and molecular clusters (Doye et al., 2004; Leary, 2000; Lyakhov, Oganov, Stokes and Zhu, 2013). However, finding the lowest-energy configuration of N particles on the unit sphere is a constrained optimization problem that is difficult for popular local optimization methods like the L-BFGS method (Liu and Nocedal, 1989). To circumvent this difficulty, we follow the idea of (Mehta et al., 2015; Wales and Ulker, 2006) and convert this constrained optimization problem into an unconstrained optimization problem which can be conveniently tackled with local optimization methods. The unconstrained optimization problem is obtained by the following spherical coordinate transformation:

$$\begin{cases} x = \sin\varphi\cos\theta; & (3) \\ y = \sin\varphi\sin\theta; & (4) \\ z = \cos\varphi; & (5) \end{cases}$$

where (x, y, z) and (φ, θ) represent respectively the cartesian coordinates and the spherical coordinates of a particle r on the unit sphere.

Thus, using the spherical coordinates, the potential function of the Thomson problem defined by Eq. (1) can be written as:

$$E_{Th}(\varphi, \theta) = \sum_{i=1}^{N-1} \sum_{j=i+1}^N \frac{1}{(2 - 2\sin\varphi_i\sin\varphi_j\cos(\theta_i - \theta_j) - 2\cos\varphi_i\cos\varphi_j)^{1/2}} \quad (6)$$

and the discrete logarithmic potential defined by Eq. (2) can be written as:

$$E_{Log}(\varphi, \theta) = -\frac{1}{2} \sum_{i=1}^{N-1} \sum_{j=i+1}^N \log(2 - 2\sin\varphi_i\sin\varphi_j\cos(\theta_i - \theta_j) - 2\cos\varphi_i\cos\varphi_j) \quad (7)$$

where $\varphi = (\varphi_1, \varphi_2, \dots, \varphi_N) \in R^N$, $\theta = (\theta_1, \theta_2, \dots, \theta_N) \in R^N$.

It is easy to observe from Eqs. (6) and (7) that in the spherical coordinate system the minimization of both the Coulomb and logarithmic potentials is an unconstrained global optimization problem with $2N$ variables, where N is the number of particles. It should be noted that the converted problems Eqs. (6) and (7) are equivalent to the original problems given by Eqs. (1) and (2), respectively, i.e., the global and local minima of the original problems do not change under the unconstrained formulations. Thus, the proposed algorithm employs Eqs. (6) and (7) as its evaluation functions f to measure the fitness of each candidate solution, where a candidate solution denoted by $(\varphi_1, \theta_1, \varphi_2, \theta_2, \dots, \varphi_2, \theta_2)$ corresponds to a configuration of N particles on the unit sphere S^2 .

Algorithm 1: General procedure of the hybrid evolutionary algorithm

Input: Number of particles to be distributed (N), maximum time limit (t_{max}), the search depth (β), precisions for the local search method $\{\epsilon_1, \epsilon_2\}$
Output: The best configuration found (S^*)

```

1 ( $POP, \Delta_f$ )  $\leftarrow$  InitialPopulation()                               /* Algorithm 2 */
2  $S^* \leftarrow \operatorname{argmin}\{f(s) : s \in POP\}$ 
3 while  $time() \leq t_{max}$  do
4    $NoImprove \leftarrow 0$ 
5   while  $NoImprove \leq \beta \wedge time() \leq t_{max}$  do
6      $S \leftarrow \operatorname{RandomlySelect}(POP)$ 
7      $S \leftarrow \operatorname{Perturbation}(S)$                                /* Algorithm 4 */
8     /* Two-phase local optimization */
9      $S \leftarrow \operatorname{LocalOptimization}(S, \epsilon_1)$ 
10    if  $f(S) < f(S^*) + 1.5 \times \Delta_f$  then
11      |  $S \leftarrow \operatorname{LocalOptimization}(S, \epsilon_2)$ 
12    end
13    PopulationUpdate( $S, POP$ )                                       /* Algorithm 5 */
14    if  $f(S) < f(S^*)$  then
15      |  $S^* \leftarrow S$                                              /* Save the best solution found */
16      |  $NoImprove \leftarrow 0$ 
17    else
18      |  $NoImprove \leftarrow NoImprove + 1$ 
19    end
20  end
21   $POP \leftarrow \operatorname{RebuildPopulation}(POP)$                        /* Algorithm 3 */
22 end
23 return  $S^*$ 

```

2.2. General approach

The proposed HEA algorithm consists of five components: population initialization, population rebuilding, two-phase local optimization, perturbation, and population updating. In fact, the HEA algorithm shares the similar spirit with the popular population-based basin-hopping (PBH) algorithm (Grosso et al., 2007), but differs from the PBH algorithm by its early-stopping strategy, the population rebuilding strategy, and the distance function that measures the difference between solutions. The pseudo-code of the algorithm is given in Algorithm 1, where POP is the current population, and S and S^* are the current solution and the best solution found so far, respectively.

The algorithm starts from the initial population (line 1) and performs two nested 'while' loops until the time limit t_{max} is reached (lines 3–21). At each iteration of the outer 'while' loop, the algorithm first improves the population using the inner 'while' loop until the search stagnates and the population converges (lines 5–19), i.e., the best solution S^* cannot be further improved during β consecutive perturbations in the inner 'while' loop, where β is a parameter called the search depth. Then, to diversify the search, the algorithm rebuilds the population while keeping a part of high-quality solutions in the new population (line 20).

At each iteration of the inner 'while' loop, the algorithm first selects randomly an individual from the population POP as the parent solution and then mutates it by a perturbation operator (lines 6–7). Subsequently, the perturbed solution is improved by the two-phase local optimization (lines 8–11). Specifically, the perturbed solution S is improved by the local optimization with a low precision ϵ_1 (line 8). This solution is further improved by the local optimization procedures with a high precision ϵ_2 if it is identified as a very promising solution (i.e., $f(S) < f(S^*) + 1.5 \times \Delta_f$), where S^* is the best solution found so far and Δ_f is the average difference between the objective values of solutions obtained by the local optimization with precisions ϵ_1 and ϵ_2 in the initial population. With the help of this two-phase optimization technique, non-promising candidate solutions will be ignored by the second local optimization phase, thus largely saving the computational effort and speeding up the search. Finally, the resulting

solution from the local optimization is used to update the population *POP* by a distance-based population updating strategy (line 12).

2.3. Local optimization method

As its local optimization component, the algorithm employs a limited-memory quasi-Newton method (Liu and Nocedal, 1989) called the L-BFGS algorithm, which is known as one of the most efficient local optimization methods for unconstrained optimization with the first derivative. The stopping criterion of the L-BFGS method is that the maximum norm $\|g\|_\infty$ of the gradient $g(X)$ of the objective function $E(X)$ is smaller than a given precision ϵ (i.e., $\|g\|_\infty \leq \epsilon$). Note that the current L-BFGS algorithm uses a line search method from (Hager and Zhang, 2005, 2013) to determine the step size of each iteration.

In addition, it should be mentioned that our algorithm performs the L-BFGS algorithm in a two-phase fashion to accelerate the search process and avoid unnecessary computational effort (i.e., performing the local optimizations from the promising points). At the first phase, a low precision ϵ_1 is used as an early-stopping condition. Then, the second phase is performed using a high precision ϵ_2 to further raise the solution quality if and only if the solution returned by the first phase is identified as a promising candidate solution (see Section 2.2 for the criterion of high-quality solutions). In Section 5.2, we experimentally verify the merit of this two-phase local optimization with the early-stopping strategy.

It is worth noting that the two-phase optimization strategy is a very general heuristic and can be applied to a number of global optimization problems, such as the sphere packing problem and the structural optimization of atomic clusters (Addis, Locatelli and Schoen, 2008; Doye et al., 2004).

2.4. Population initialization and regeneration

To obtain an initial population *POP* composed of np individuals (solutions) at the different stages of the algorithm, the proposed algorithm employs two methods. At the beginning, the algorithm uses the first method described in Algorithm 2 to generate the initial population, where each solution in *POP* is created by distributing randomly the N particles on the surface of unit sphere S^2 and then improving it by the local optimization method. It should be noted that an individual in the population is denoted by $(\varphi_1, \theta_1, \varphi_2, \theta_2, \dots, \varphi_N, \theta_N)$ using the spherical coordinate system in order to facilitate the local optimization of the objective function, where (φ_i, θ_i) represents the coordinate of particle r_i . At this stage, for each solution in *POP*, local optimization is performed with different precisions ϵ_1 and ϵ_2 to improve its quality, and the objective difference Δ_f between the resulting solutions is recorded and then applied by the subsequent two-phase local optimization to speed up the search process.

When the population converges and the search stagnates, the algorithm employs the second initialization method to rebuild the population, while keeping several high-quality solutions in the new population. Concretely, the individuals in the population are first sorted according to their objective values, and the first $\alpha \times np$ best individuals are kept in the population, where α is a parameter which is empirically set to 0.2. Then each remaining individual is regenerated by distributing randomly the N particles on the surface of the unit sphere and is further improved by the local optimization. The pseudo-code of rebuilding the population is provided in Algorithm 3.

2.5. Perturbation method

To jump out of the local optimal traps, the algorithm employs a random perturbation operator to change the current solution. The pseudo-code of the perturbation is given in Algorithm 4. Given a candidate solution indicated by the spherical coordinate $(\theta_1, \varphi_1, \theta_2, \varphi_2, \dots, \theta_N, \varphi_N)$, the perturbation operator shifts each coordinate of the candidate solution in the interval $[-\eta, \eta]$ to produce a new offspring solution (lines 3–4), where $\eta = \eta_0 \times \theta_{min}$ is called the perturbation strength with η_0 being a parameter and $\theta_{min} = \text{Min}_{i < j} \{\arccos(\vec{r}_i \cdot \vec{r}_j)\}$ being the minimum angle between two particles (\vec{r}_i and \vec{r}_j represent respectively the cartesian coordinates of particles r_i and r_j).

2.6. Population updating strategy

When a local minimum solution is returned by the local optimization, the algorithm employs a distance-based population updating (DPU) strategy to determine how the population is updated. Following (Hao, 2012; Grosso et al., 2007), the DPU strategy aims to not only maintain high-quality solutions in the population, but also keep a suitable population diversity. The pseudo-code of the DPU strategy is provided in Algorithm 5.

Given an offspring solution S_{off} and the current population *POP*, the DPU strategy first identifies the worst solution S_w in *POP* and the closest solution S_c to S_{off} (lines 2–4). Then, the average distance (D_{avg}) between

Algorithm 2: Population initialization method

```

1 Function InitialPopulation()
   Input: Size of population ( $np$ ), the precisions of local search  $\{\epsilon_1, \epsilon_2\}$ 
   Output: The initial population  $POP$ , the average objective difference between the solutions obtained by two
             local searches with different precisions ( $\Delta_f$ )
2  $\Delta_f \leftarrow 0$ 
3 for  $k \leftarrow 1$  to  $np$  do
4   for  $i \leftarrow 1$  to  $N$  do
5      $POP[k].\theta_i \leftarrow rand(0, \pi)$           /*  $rand(0, \pi)$  denotes a random number in  $(0, \pi)$  */
6      $POP[k].\varphi_i \leftarrow rand(0, 2\pi)$ 
7   end
8    $f_1 \leftarrow LocalOptimization(POP[k], \epsilon_1)$ 
9    $f_2 \leftarrow LocalOptimization(POP[k], \epsilon_2)$ 
10   $\Delta_f \leftarrow \Delta_f + (f_1 - f_2)/np$ 
11 end
12 return  $\{POP, \Delta_f\}$ 
    
```

Algorithm 3: Population rebuilding method

```

1 Function RebuildPopulation()
   Input: Input population  $POP$ , size of population ( $np$ ), parameter  $\alpha$ , precision of local search ( $\epsilon_1$ )
   Output: New population  $POP$ 
2 QuickSort( $POP$ ) /* Sort the individuals in  $POP$  according to their objective
                    values in a descending order */
3 for  $k \leftarrow 1$  to  $(1 - \alpha) \times np$  do
4   for  $i \leftarrow 1$  to  $N$  do
5      $POP[k].\theta_i \leftarrow rand(0, \pi)$ 
6      $POP[k].\varphi_i \leftarrow rand(0, 2\pi)$ 
7   end
8    $LocalSearch(POP[k], \epsilon_1)$ 
9 end
   /* The first  $\alpha \times np$  best individuals of input population are kept in the
      new population */
10 return  $POP$ 
    
```

the solutions in the population is calculated (line 5) and POP is updated as follows. If S_{off} is better than S_c and the distance between S_{off} and S_c is smaller than $d_{cut} \times D_{avg}$, where d_{cut} is a parameter, S_{off} replaces the closest solution S_c (lines 6–7). If $E(S_{off}) < E(S_w)$ and the distance between S_{off} and S_c is larger than $d_{cut} \times D_{avg}$, S_{off} replaces the worst solution S_w in the population (lines 8–9). The population is kept unchanged in other cases.

The distance metric between solutions is a key issue for geometry optimization problems since geometrical configurations of solutions can be rotated arbitrarily and do not change in essence. In this study, to deal with the minimum-energy configuration problem on the sphere, we use the energies of particles to define the distance between solutions, which differs from the popular strategies in the literature that use the information of coordinates or neighbors of particles to define the distance between solutions. Given two solutions S_a and S_b (i.e., two configurations of N particles on the unite sphere), the distance between them is calculated in the following three steps. First, we calculate the energy $e(i)$ of each particle r_i for each of two solutions as follows:

$$e(i) = \sum_{j \neq i} e(i, j) \quad (8)$$

Algorithm 4: Perturbation method

```

1 Function Perturbation()
  Input: Input solution ( $S$ ), the perturbation strength ( $\eta$ )
  Output: Perturbed solution  $S$ 
2 for  $i \leftarrow 1$  to  $N$  do
3    $S.\theta_i \leftarrow S.\theta_i + \text{rand}(-\eta, \eta)$       /*  $\text{rand}(-\eta, \eta)$  denotes a random number in  $(-\eta, \eta)$  */
4    $S.\varphi_i \leftarrow S.\varphi_i + \text{rand}(-\eta, \eta)$ 
5 end
6 return  $S$ 
    
```

Algorithm 5: Population updating method

```

1 Function PopulationUpdate()
  Input: Offspring solution  $S^o$ , population  $POP$ , distance cutoff factor  $d_{cut}$ 
  Output: Updated population  $POP$ 
2  $S_w \leftarrow \text{argmax}\{E(S) : S \in POP\}$       /*  $S_w$  denotes the worst solution in  $POP$  */
3  $S_c \leftarrow \text{argmin}\{\text{distance}(S, S_{off}) : S \in POP\}$  /*  $S_c$  denotes the closest solution to  $S^o$ 
   in  $POP$  */
4  $d_{min} \leftarrow \text{distance}(S_c, S_{off})$       /*  $d_{min}$  is the distance between  $S^o$  and  $S_c$  */
5  $D_{avg} \leftarrow \frac{\sum_{i < j} \text{distance}(POP[i], POP[j])}{np(np-1)/2}$  /*  $D_{avg}$  denotes the average distance between
   solutions in  $POP$  */
6 if  $(E(S_{off}) < E(S_c)) \wedge (d_{min} \leq d_{cut} \times D_{avg})$  then
7    $POP \leftarrow POP \cup \{S_{off}\} \setminus \{S_c\}$ 
8 else if  $E(S_{off}) < E(S_w) \wedge (d_{min} > d_{cut} \times D_{avg})$  then
9    $POP \leftarrow POP \cup \{S_{off}\} \setminus \{S_w\}$ 
10 end
11 return  $POP$ 
    
```

where $e(i, j)$ represents the energy between particles r_i and r_j and is defined as $\frac{1}{\|r_i - r_j\|}$ and $\log \frac{1}{\|r_i - r_j\|}$ in which $\|r_i - r_j\|$ denotes the Euclidean distance between the particles r_i and r_j for the Coulomb and logarithmic potentials, respectively. Then, the energies $\{e(1), e(2), \dots, e(N)\}$ of the N particles are sorted in an ascending order for S_a and S_b respectively. Finally, the distance between S_a and S_b is defined by:

$$\text{distance}(S_a, S_b) = \sum_{i=1}^N |e_a(i) - e_b(i)| \quad (9)$$

As indicated in Section 2.4, a candidate solution S and a particle r_i in S are represented as $(\varphi_1, \theta_1, \varphi_2, \theta_2, \dots, \varphi_N, \theta_N)$ and (φ_i, θ_i) respectively, using the spherical coordinate system. Thus, to calculate the Euclidean distance $\|r_i - r_j\|$ between two particles r_i and r_j , the spherical coordinates of the particles are first transformed into their Euclidean coordinates (x_i, y_i, z_i) and (x_j, y_j, z_j) .

2.7. Discussions

The proposed HEA algorithm shares some similarities with the popular PBH algorithm (Grosso et al., 2007) and can be considered as an extended variant of PBH. However, HEA differs from the PBH algorithm in the following aspects. First, the proposed algorithm uses a two-phase local optimization method with an early-stopping strategy to speed up the search process. Second, when the population converges and the search stagnates, the proposed algorithm employs a population rebuilding strategy to maintain a healthy population, while retaining several elite individuals in the new population. Third, the proposed algorithm uses an energy-based distance function to measure the difference between solutions. As we show in the experimental study in the next section, the proposed HEA algorithm performs

remarkably well when it is applied to solve a large number of instances of the minimum energy configuration problems with the Coulombic potential and the discrete logarithmic potential on the unit sphere.

3. Experimental Evaluation

We evaluate the performance of the proposed HEA algorithm on a set of benchmark instances widely used in the literature.

3.1. Parameter settings and experimental protocol

The HEA algorithm employs several parameters whose default settings were empirically determined by a preliminary experiment and were described in Table 1. In this study, all computational experiments were executed with the default settings of parameters.

The HEA algorithm¹ was implemented in the C++ language and all computational experiments in this study were executed on a computer with an Intel(R) Xeon (R) Platinum 9242 CPU (2.3 GHz), running a Linux operating system. To assess the average performance of our algorithm, we employed 20 Thomson instances in the range of $300 \leq N \leq 500$ as our test bed and ran the algorithm 5 times to solve each instance. Moreover, to locate the global minimum configuration for the discrete logarithmic potential, we ran the HEA algorithm 5 times on each instance with $N \leq 500$ and several large instances with $N > 500$. The stopping condition of the algorithm is a maximum time limit t_{max} whose settings depend on N and are shown in Table 2.

3.2. Computational Assessment on the Coulomb potential

In order to verify whether the proposed algorithm is able to locate global minimum solutions in general cases for different problem instances and to preliminarily evaluate the performance of the algorithm, we conducted an experiment based on a set of 20 selected Thomson instances with the Coulomb potential and made a comparison between our results and the best-known solutions reported in the literature and publicly available on the Cambridge Cluster Database (Wales, 2022). It is worth noting that the best-known solutions of these instances were obtained by the popular basin-hopping algorithm and extensive computational experiments in previous studies (Wales and Ulker, 2006; Wales et al., 2009), under a stopping condition of up to 10^5 local optimization steps per run. According to (Wales and Ulker, 2006), if these best-known solutions are not global minima, they are close enough to the global minima for structural analysis to be relevant. These lowest energy solutions are generally difficult to find, and this is especially true when $N > 300$.

The computational results of the HEA algorithm over 5 runs are summarized in Table 3. The first two columns give the number of particles (N) and the best-known result (BKR) in the literature, and the results of our HEA algorithm are reported in the last five columns, including the best objective value over 5 runs (E_{best}), the average objective value (E_{avg}), the worst objective value (E_{worst}), the standard deviation of objective values obtained (σ), and the average computational time (time(s)) in seconds to reach its final result. Row '#Better/#Equal/#Worse' indicates the number of instances for which our HEA algorithm obtained a better, equal or worse result compared to the best-known result in the literature.

Table 3 shows that the proposed HEA algorithm is able to find the best-known results for all 20 instances tested except for $N = 380, 460$ with small standard deviations $\sigma \leq 0.05$. These results were found under much less generous time limits (e.g., 3×10^4 local optimization steps for HEA against 10^5 local optimization steps for previous studies (Wales and Ulker, 2006; Wales et al., 2009)). To reach its best results, HEA requires no more than 3 hours on our 2.3 GHz computer. The results of this experiment ensure the validity of the structural analysis of configurations in the following section.

Finally, we mention that we have also tested the proposed algorithm on the general Riesz s -energy function defined in Section 1 (Eq. (1)) when $s = 2$. The results showed that our algorithm performs similarly to the cases with the Coulombic potential ($s = 1$) and the discrete logarithmic potential (s tends to 0). That is, the algorithm can consistently find the best-known solutions for all tested instances from the literature (Ridgway and Cheviakov, 2018).

¹The the program codes of our algorithm and the best solutions found in this work will be available at <https://github.com/XiangjingLai/minimum-energy-configurations>

Table 1
Settings of parameters

Parameters	Section	Description	Values
β	2.2	search depth	500
ϵ_1	2.4	precision of local optimization	10^{-2}
ϵ_2	2.4	precision of local optimization	10^{-5}
np	2.4	size of population	50
α	2.4	parameter for population rebuilding	0.2
η_0	2.5	parameter to control perturbation strength	0.5
d_{cut}	2.6	coefficient used in population updating	0.5

Table 2
Summary of the maximum time limits used

N	$t_{max}(s)$	N	$t_{max}(s)$
$N \leq 100$	200	$301 \leq N \leq 350$	200×2^5
$101 \leq N \leq 150$	200×2	$351 \leq N \leq 400$	200×2^6
$151 \leq N \leq 200$	200×2^2	$401 \leq N \leq 450$	200×2^7
$201 \leq N \leq 250$	200×2^3	$451 \leq N \leq 500$	200×2^8
$251 \leq N \leq 300$	200×2^4	$N > 500$	10^5

Table 3
Computational results and comparison on 20 representative Thomson instances in the range of $300 \leq N \leq 500$. In terms of E_{best} , results equaling the best-known values (BKR) in the literature are indicated in bold.

N	BKR	E_{best}	E_{avg}	E_{worst}	σ	time(s)
310	45036.4985723	45036.4985723	45036.4985723	45036.4985723	0.000000	156
320	48039.4689302	48039.4689302	48039.4689303	48039.4689303	0.000000	1238
330	51140.0513603	51140.0513603	51140.0513603	51140.0513604	0.000000	457
340	54338.4944598	54338.4944598	54338.5013247	54338.5287839	0.013730	1606
350	57634.5963953	57634.5963953	57634.5963953	57634.5963953	0.000000	662
360	61028.5522272	61028.5522272	61028.5522272	61028.5522273	0.000000	1110
370	64520.0471868	64520.0471868	64520.0471868	64520.0471868	0.000000	646
380	68109.8676249	68109.8676249	68109.8676250	68109.8676250	0.000000	3725
390	71797.0353361	71797.0353361	71797.0522364	71797.1198380	0.033801	2400
400	75582.4485123	75582.4485123	75582.4487417	75582.4496592	0.000459	3886
410	79465.7432086	79465.7432086	79465.7432086	79465.7432086	0.000000	3092
420	83446.9975990	83446.9975990	83446.9994932	83447.0023344	0.002320	5440
430	87526.1187029	87526.1187029	87526.1187029	87526.1187029	0.000000	2893
440	91703.3295563	91703.3295563	91703.3554818	91703.3776659	0.021337	1349
450	95978.4413763	95978.4413763	95978.4563615	95978.5163022	0.029970	2936
460	100351.7631087	100351.7671579	100351.7806085	100351.7880156	0.007636	4836
470	104822.8863243	104822.8863243	104822.8863243	104822.8863244	0.000000	8516
480	109392.3186786	109392.3186786	109392.3387663	109392.4191169	0.040175	7444
490	114059.8425562	114059.8425562	114059.8582967	114059.8622319	0.007870	5683
500	118825.4625422	118825.4625422	118825.4625422	118825.4625422	0.000000	8426
#Better/#Equal/#Worse		0/18/2				

4. Structural Analysis and Comparison of Two Studied Potentials

In this section, we turn to an analysis and comparison of the putative optimal configurations for the two classic potentials, i.e., the Coulomb and discrete logarithmic potentials. Particularly, we will focus on the results of logarithmic potential because few experimental result is available in the present literature for this potential.

4.1. Comparison between the putative optimal configurations of the two potentials

The putative optimal configurations of the Thomson problem with the Coulombic potential have been widely investigated in the literature. In particular, all putative optimal configurations of the Thomson problem are online available at the Cambridge energy landscape database (Wales, 2022) for $N \leq 400$. However, the studies for the putative optimal configurations of the logarithmic potential is very scarce in the literature, although the logarithmic

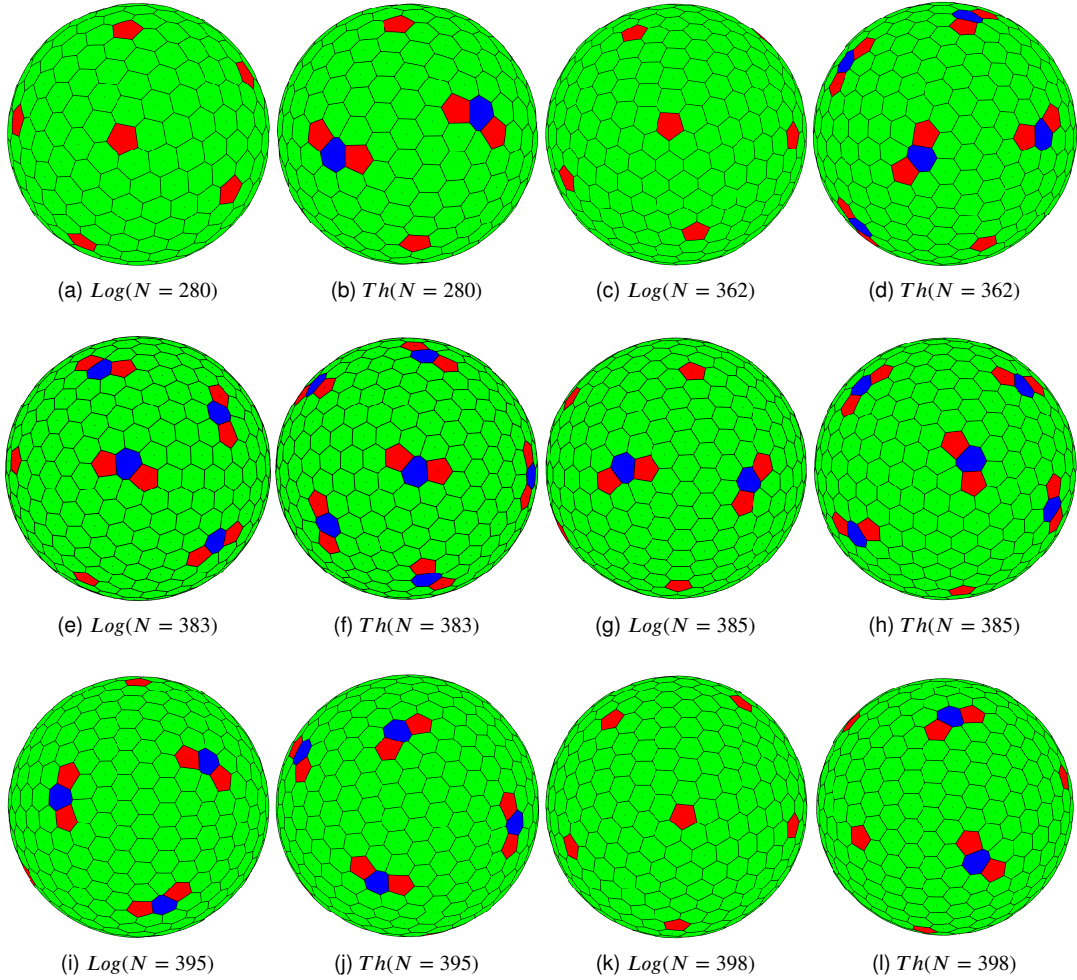


Figure 1: Comparison between the putative global minima for logarithmic and Coulombic potentials on several representative instances.

potential is much more widely investigated in mathematics than the Coulombic potential. This section aims to make a systematical comparison between the best-known configurations of the logarithmic and Coulombic potentials for $N \leq 400$.

By carefully comparing the best-known configuration of the Coulombic potential and the best configuration found in this work for the logarithmic potential, we have an interesting finding that these two potentials have the same best configuration for all but 43 instances in this range, which means that these two potentials have a high similarity in the ground-state configurations.

For the 43 instances for which the best configurations differ for the two potentials, the comparative results are summarized in Table 4. The first two columns give the size N and the best result found in this work for the logarithmic potential, the third column shows the energy of the configuration corresponding to the result of column 2 in terms of the Coulombic potential, and the fourth column indicates the best-known result for the Coulombic potential. One can observe two phenomena from Table 4. First, for these 43 sizes, the best-known configuration of the logarithmic potential also corresponds to a very low energy in the Coulombic potential after a local optimization, which is very close to the best-known result of the Thomson problem with the Coulombic potential as its potential function. Second, the number of instances for which the two potentials have different best-known configurations rapidly increases as N increases.

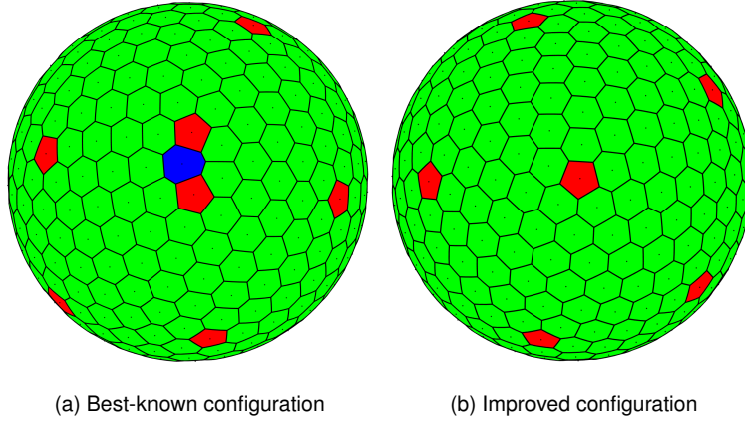


Figure 2: Best-known configuration ($E = 61028.5522271$) and the improved configuration ($E = 61028.5290983$) for the Thomson problem with $N = 360$.

To have an intuitive impression for the best-known configurations of the two potentials and the differences between them, we give in Fig. 1 a Voronoi representation of the best-known configurations of six selected sizes for the two potentials, where the configurations for the logarithmic and Coulombic potentials are marked by ‘Log’ and ‘Th’, respectively. For the current Voronoi representation with N particles, the spherical surface S^2 is partitioned to N disjoint cells C_1, C_2, \dots, C_N , where each cell C_i corresponds to a particle r_i and a polygon which is colored according to its number of edges. Formally, a cell C_i on S^2 is defined as follows (Saff and Kuijlaars, 1997):

$$C_i = \{r \in S^2 : \|r - r_i\| = \min_{1 \leq k \leq N} \|r - r_k\|\} \quad (10)$$

To identify the difference between spherical configurations, we focus on an important feature, i.e., the topological defects whose nature and concentration govern a number of characteristics such as mechanical strength, electrical conductivity, optical properties, and crystal growth rates (Wales and Ulker, 2006). In fact, an alveolate packing of cells is very perfect, where all cells are hexagonal (i.e., all particles have six nearest neighbors). However, according to Euler’s theorem, it is impossible that all cells of a spherical configuration are hexagonal. In other words, it is inevitable that there exist a number of quadrilateral, pentagonal and heptagonal cells. Thus, these non-hexagonal cells and their combinations are considered as the topological defects of configuration and are widely used to characterize spherical configurations in the previous studies (Pérez-Garrido, Dodgson, Moore, Ortuno and Diaz-Sanchez, 1997; Wales and Ulker, 2006; Wales et al., 2009). Concretely, a topological defect on the configuration can be defined as a building block of one or several adjacent non-hexagonal cells.

Fig. 1 shows that the best-known configuration generally has more large defects with the Coulombic potential than with the logarithmic potential for the same size N , which indicates the difference between the two potentials on the ground-state configurations.

In addition, by comparing the best results of the two potentials for $N \leq 400$, we find that the best configuration of the logarithmic potential is consistent with that of the Coulombic potential for $N = 360$. However, the energy of this configuration is lower than the best-known result in the literature for the Coulombic potential, which means that we discovered an improved solution for the classic Thomson problem with $N = 360$. The Voronoi representations of our improved solution and the previous best-known solution are given in Fig. 2, which shows that the improved solution has less defects than the best-known solution.

For the Coulombic potential with $N = 360$, a great deal of computational effort has been used to search for its global minimum solution in the literature, without finding the newly improved solution. According to the energy landscape theory (Doye et al., 1999), the potential energy surface (PES) of the instance $N = 360$ of the Thomson problem contains several competing funnels and the global minimum solution lies in a very narrow and deep funnel which is separated from other main funnels. This feature makes it highly challenging to find the global minimum solution or high-quality local minimum solutions that are better than the best-known solution. Therefore, the new

Table 4Energies of the instances for which the two potential functions have different best-known structures for $N \leq 400$.

N	Logarithmic	Coulombic	Coulombic (BKR)
56	-360.5458992	1337.0953483	1337.0949452
66	-491.4074700	1882.4420928	1882.4415253
74	-610.2670714	2387.0751671	2387.0729818
78	-674.4529942	2662.0472133	2662.0464745
86	-812.1513219	3258.2136631	3258.2116057
116	-1440.2584652	6038.8177466	6038.8155935
148	-2304.0197787	9958.4093391	9958.4060042
170	-3013.6050764	13226.6832018	13226.6810785
174	-3152.7500821	13871.1972776	13871.1870922
180	-3367.2916249	14867.1007295	14867.0999275
185	-3551.4181659	15723.7234640	15723.7200740
201	-4173.3330628	18627.5937862	18627.5912262
213	-4672.4221235	20968.6246256	20968.6120254
242	-5994.0776103	27203.8047199	27203.7992855
254	-6588.7453491	30023.2299430	30023.2228618
266	-7211.3610485	32982.9968124	32982.9836290
270	-7425.1185679	34000.6713597	34000.6484970
276	-7751.5583417	35556.6376953	35556.6333035
278	-7861.9297921	36083.0479253	36083.0368937
280	-7973.0836085	36613.2764627	36613.2695900
285	-8254.3317922	37956.2416239	37956.2394559
300	-9127.2018542	42131.2793896	42131.2641372
300	-9127.2018542	42131.2793896	42131.2641372
337	-11466.8895186	53368.7673341	53368.7548248
343	-11871.3240914	55317.0136221	55317.0070681
347	-12144.8182601	56635.4452758	56635.4365234
350	-12351.9680192	57634.6050414	57634.5963952
362	-13198.0331124	61719.0635127	61719.0519098
365	-13413.9201422	62762.0622093	62762.0612627
374	-14072.0147608	65944.3457085	65944.3296990
378	-14369.5358077	67384.1456614	67384.1420018
379	-14444.4041714	67746.5263921	67746.5082391
380	-14519.4685446	68109.8638631	68109.8414480
382	-14670.1670602	68839.4910273	68839.4702441
383	-14745.8127442	69205.7623724	69205.7419857
384	-14821.6521209	69573.0133653	69572.9897864
385	-14897.6858630	69941.2368800	69941.2195535
386	-14973.9129191	70310.4439019	70310.4221247
387	-15050.3346329	70680.6245253	70680.6036344
388	-15126.9473389	71051.7710529	71051.7709033
393	-15512.8973379	72922.5689915	72922.5410777
394	-15590.6697432	73299.6554482	73299.5933286
395	-15668.6380476	73677.6500641	73677.6284822
398	-15903.7118903	74817.6118481	74817.5835941

record-breaking solution for the case $N = 360$, which reduces the defects compared to the best-known solution, can be considered as a remarkable result.

4.2. Structural evolution of the putative optimal configurations for the discrete logarithmic potential

Systematical studies about the putative optimal configurations of the logarithmic potential is still scarce, although a large number of theoretical researches have been reported in the literature. In this section, we investigate the structural distribution and evolution of the putative optimal configurations for the logarithmic potential. We also make the best solutions found in this work available at the webpage indicated in footnote 1.

We checked the best configuration found for each instance for $N \leq 500$ and found that the best configurations of most instances exhibit an icosahedral configuration with 12 disclinations and a number of defects (≤ 12). Nevertheless, we also found some other types of configurations which are given in Fig. 3 especially for small instances with $N \leq 250$. It should be mentioned that the best configurations in Fig. 3 are the same as the putative optimal solutions of the Thomson problem in (Wales and Ulker, 2006) except for $N = 174$.

To have an intuitive impression for the structural evolution of the best configurations for medium-sized instances, we give in Fig. 4 the Voronoi representation of the best configuration for several representative instances in the range $350 \leq N \leq 500$. One observes from Fig. 4 that for these medium-sized instances, the best configurations exhibit an icosahedral configuration with several disclinations and/or defects.

Moreover, to further show the best configurations for large instances, we also give in Fig.4 the Voronoi representation of the best solution for 4 representative instances with $N = 942, 1500, 1152$ and 2000. We observe

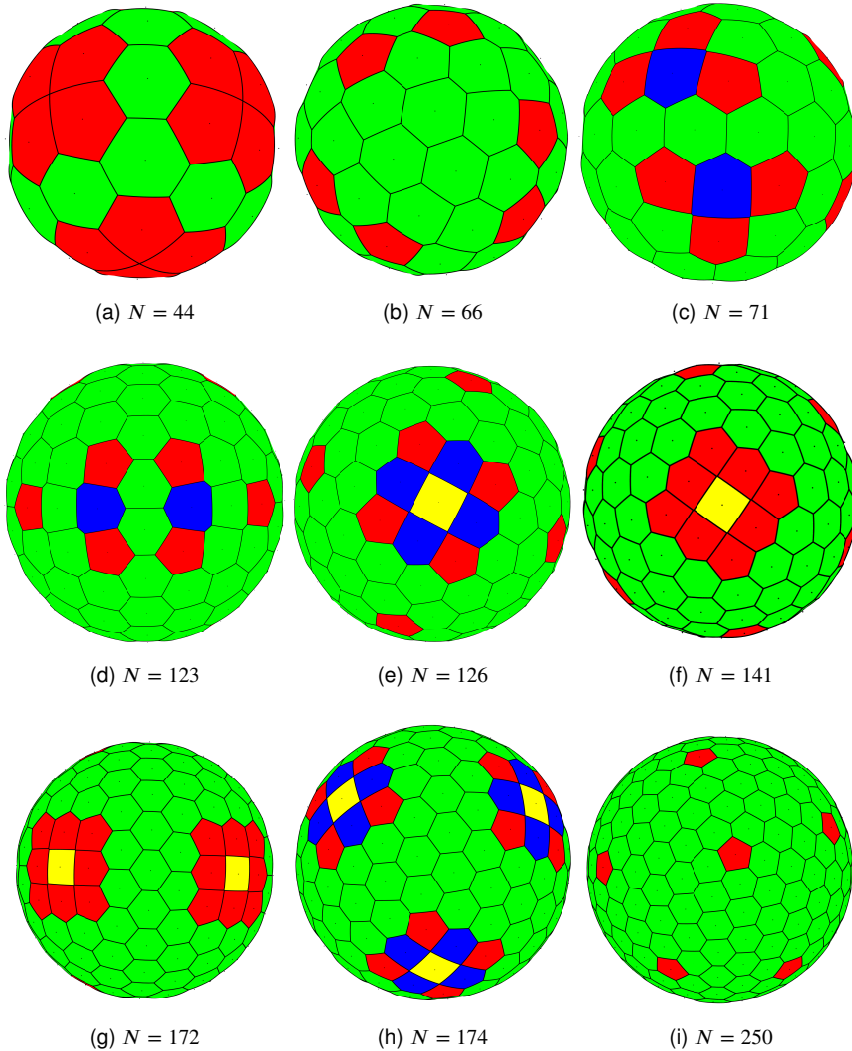


Figure 3: Best configurations found for representative instances with the logarithmic potential for $N \leq 250$.

from the figure that these configurations are very similar to the best-known configurations of the Thomson problem in (Wales et al., 2009). For example, for $N = 942$ and 1152 , the best configuration contains two types of defects, where the first type of defects consist of one heptagon and two pentagons and the second type of defects consist of two heptagons and three pentagons. For the larger instances with $N = 1500$ and 2000 , the best configuration contains several ‘rosette’ defects and irregular boundaries composed of several small defects.

In summary, these observations indicate that the putative optimal configurations of the most tested instances for the logarithmic potential have the same structural features as those of the Thomson problem (Wales et al., 2009) and that the energy of icosahedral configurations can be reduced by introducing a number of disclinations or defects especially for large instances.

4.3. Energy distribution of particles for the putative optimal solutions of logarithmic potential

To have an intuitive impression for the energy distribution of particles, we give in Fig. 5 the colored Voronoi representation for the putative optimal configurations of several representative instances with the logarithmic potential, where the cells are colored according to the energies $e(i)$ of the corresponding particles calculated by Eq. (8). Thus the colors of cells vary gradually according to the energies of particles. Particularly, a crimson cell means a high-energy particle and a navy-blue cell means a low-energy particle.

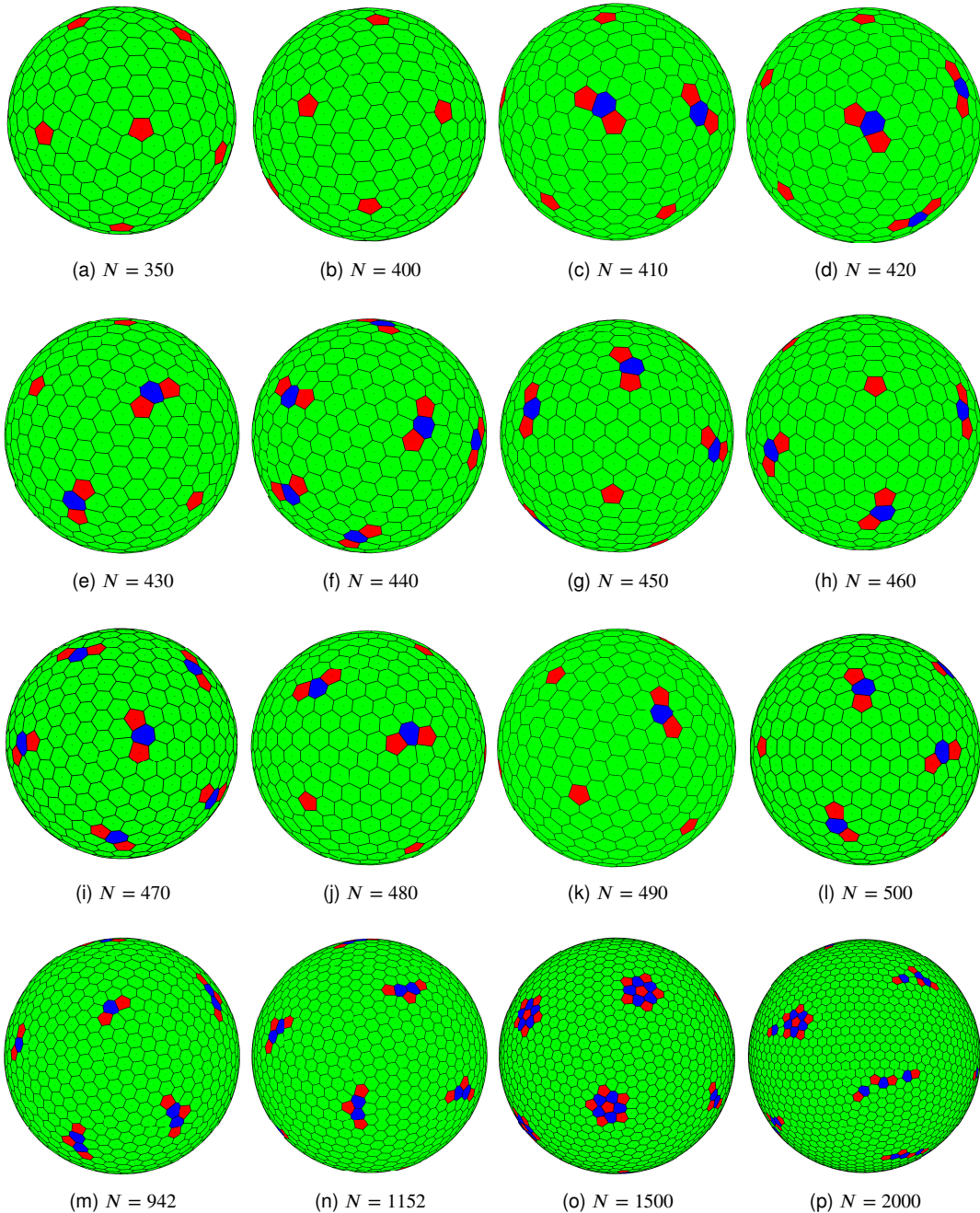


Figure 4: Best configurations found for representative instances with the logarithmic potential.

We observe from Fig. 5 that the energies of particles are distributed according to some rules. First, the highest-energy particles are always distributed in the topological defects of configuration. Second, in general cases, the energy of particle declines gradually as its distance from the topological defects increases, thus the regions far away from the topological defects are always of low energy. Third, very interestingly, the lowest-energy particles are generally located in topological defects or its vicinity for the large instances.

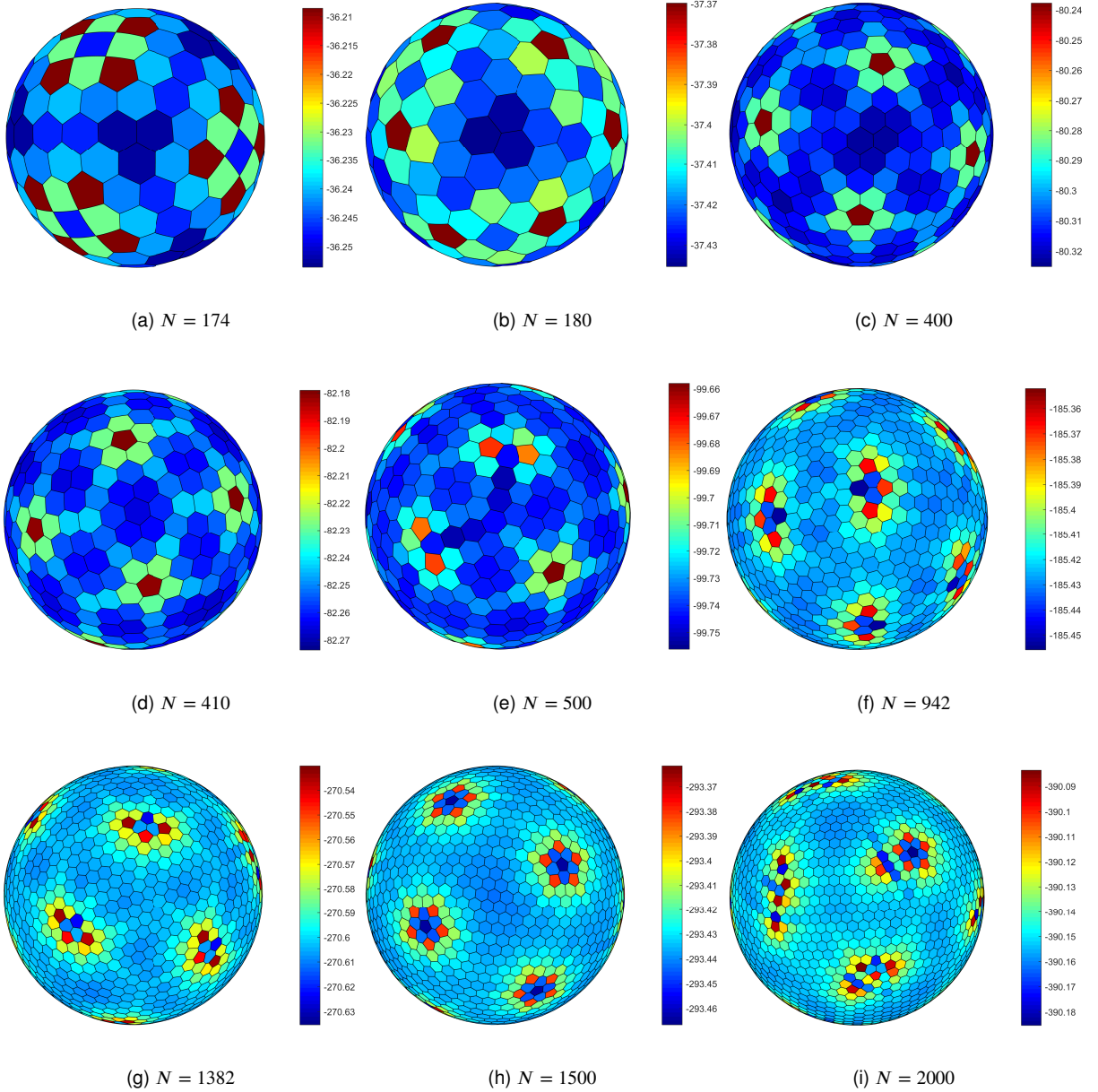


Figure 5: Energy distribution of particles on the putative optimal solutions of several representative instances with the logarithmic potential.

5. Analysis of the Key Algorithmic Components

In this section, we analyze two key components of the proposed algorithm: distance-based population updating strategy and early-stopping technique for the local optimization.

5.1. The effect of population updating strategy

To show the effect of the distance-based population updating strategy on the performance of the algorithm, we carried out an experiment based on 20 selected instances with the logarithmic potential. In the experiment, we first created a variant (denoted by HEA^-) of our HEA algorithm by replacing its population updating strategy with a

Table 5

Comparison between the distance-based population updating strategy and greedy population updating strategy in terms of E_{best} , E_{avg} and E_{worst} . Better results between two strategies are indicated in bold.

N	E_{best}		E_{avg}		E_{worst}	
	HEA ⁻	HEA	HEA ⁻	HEA	HEA ⁻	HEA
310	-9733.3772816	-9733.3772816	-9733.3772816	-9733.3772816	-9733.3772816	-9733.3772816
320	-10358.9375345	-10358.9375345	-10358.9375345	-10358.9375345	-10358.9375345	-10358.9375345
330	-11003.8979247	-11003.8979247	-11003.8979247	-11003.8979247	-11003.8979247	-11003.8979247
340	-11668.2345318	-11668.2345318	-11668.2340340	-11668.2340340	-11668.2320431	-11668.2320431
350	-12351.9680192	-12351.9680192	-12351.9679728	-12351.9680192	-12351.9677872	-12351.9680192
360	-13055.0849300	-13055.0849300	-13055.0819280	-13055.0819280	-13055.0811775	-13055.0811775
370	-13777.6040398	-13777.6040398	-13777.6040398	-13777.6040398	-13777.6040398	-13777.6040398
380	-14519.4644435	-14519.4679472	-14519.4619146	-14519.4638239	-14519.4604924	-14519.4620166
390	-15280.7584968	-15280.7584968	-15280.7553387	-15280.7565904	-15280.7427063	-15280.7489648
400	-16061.3971882	-16061.3971882	-16061.3949953	-16061.3966451	-16061.3943703	-16061.3944727
410	-16861.4133871	-16861.4133871	-16861.4124148	-16861.4133871	-16861.4085257	-16861.4133871
420	-17680.8027708	-17680.8027708	-17680.8019408	-17680.8018335	-17680.8006957	-17680.7999580
430	-18519.5847726	-18519.5847726	-18519.5847340	-18519.5847726	-18519.5845795	-18519.5847726
440	-19377.7240610	-19377.7232516	-19377.7214806	-19377.7215415	-19377.7165368	-19377.7205027
450	-20255.2463493	-20255.2463493	-20255.2457388	-20255.2459861	-20255.2442049	-20255.2454415
460	-21152.1304277	-21152.1320951	-21152.1304277	-21152.1310320	-21152.1304277	-21152.1301145
470	-22068.3996282	-22068.3996282	-22068.3948214	-22068.3973131	-22068.3891343	-22068.3957697
480	-23004.0138068	-23004.0229249	-23004.0138028	-23004.0157919	-23004.0137871	-23004.0137871
490	-23959.0124384	-23959.0165449	-23959.0080392	-23959.0123613	-23959.0026262	-23959.0053762
500	-24933.3757645	-24933.3757645	-24933.3757645	-24933.3757645	-24933.3757645	-24933.3757645
#Better		4		11		10
#Equal		15		8		8
#Worse		1		1		2

popular greedy updating strategy (Zhou, Hao and Wu, 2021) in which the worst solution in the population is replaced by the offspring if the offspring solution is different from any solution in the population and is better than the worst solution. We ran HEA and HEA⁻ 5 times on each instance. The computational results are summarized in Table 5, including the best objective value over 5 runs (E_{best}), the average objective value (E_{avg}), and the worst objective value (E_{worst}). The rows '#Better', '#Equal', '#Worse' respectively present the number of instances for which HEA obtained a better, equal or worse result compared to HEA⁻ in terms of E_{best} , E_{avg} and E_{worst} .

Table 5 shows that the HEA algorithm performs better with the distance-based population updating strategy than without it. Disabling the distance-based population updating strategy worsens the performance of the algorithm in terms of all performance indicators. This experiment indicates that the distance-based population updating strategy plays an important role for the performance of the HEA algorithm.

Moreover, to further show the effect of the distance-based population updating strategy on the diversity and convergence of population, we carried out another experiment on two representative instances, i.e., $N = 450$ and $N = 500$, where the distance-based population updating strategy and the greedy population updating strategy (i.e., the *PoolWorst* strategy) were respectively adopted in the algorithm and the average distance between solutions in the population was recorded as a function of number of iterations. The experimental results are plotted in Fig. 6.

Fig. 6 shows that the employed distance-based population updating strategy is able to maintain the diversity of solutions in the population, thus avoiding efficiently an early convergence of algorithm. In comparison, when the greedy updating strategy is adopted, the diversity of population decreases significantly as the search progresses, and thus making the population converges too early.

5.2. The effect of early-stopping strategy for local optimization

The local optimization method is the most time-consuming component of the HEA algorithm. To speed up the search process, the algorithm employs a two-phase local optimization with an early-stopping strategy to discard inferior candidate solutions that are not further improved by local optimization. To check the effectiveness of this early-stopping strategy, we created a HEA variant (denoted by HEA*) by disabling the early-stopping strategy, while

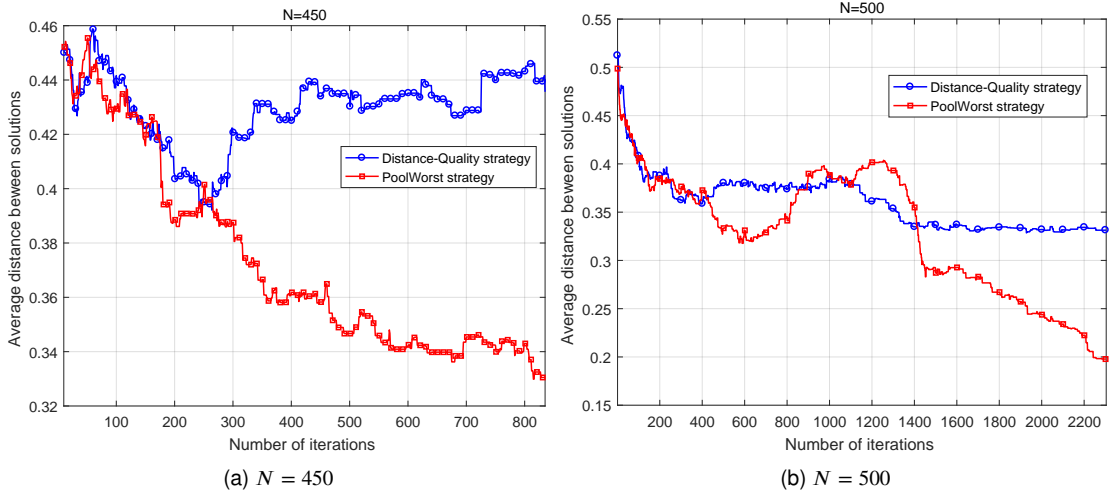


Figure 6: Comparison between the distance-based population updating strategy and the greedy population updating strategy on two representative instances with the logarithmic potential

Table 6

Comparison between the algorithms with and without the early-stopping strategy in terms of E_{best} , E_{avg} and average running time. Dominating results between the two strategies are indicated in bold.

N	E_{best}		E_{avg}		time(s)	
	HEA	HEA*	HEA	HEA*	HEA	HEA*
310	-9733.3772816	-9733.3772816	-9733.3772816	-9733.3772816	12634	29778
320	-10358.9375345	-10358.9375345	-10358.9375345	-10358.9375345	13484	29661
330	-11003.8979247	-11003.8979247	-11003.8979247	-11003.8979247	15015	29974
340	-11668.2345318	-11668.2345318	-11668.2345318	-11668.2345318	17565	36766
350	-12351.9680192	-12351.9680192	-12351.9680192	-12351.9680192	17782	37361
360	-13055.0811775	-13055.0849300	-13055.0811775	-13055.0826785	22020	43487
370	-13777.6040398	-13777.6040398	-13777.6040398	-13777.6040398	19285	42471
380	-14519.4679472	-14519.4679472	-14519.4645901	-14519.4678755	29728	55310
390	-15280.7584968	-15280.7584968	-15280.7561746	-15280.7580810	21556	53950
400	-16061.3971882	-16061.3971882	-16061.3966451	-16061.3961020	23855	54826
410	-16861.4133871	-16861.4133871	-16861.4133705	-16861.4133705	30027	56742
420	-17680.8027708	-17680.8027708	-17680.8017288	-17680.8013138	33216	64504
430	-18519.5847726	-18519.5847726	-18519.5847181	-18519.5847726	35066	60687
440	-19377.7240610	-19377.7232516	-19377.7229918	-19377.7221305	37553	71117
450	-20255.2463493	-20255.2463493	-20255.2463493	-20255.2461677	38970	72950
460	-21152.1320951	-21152.1304277	-21152.1306985	-21152.1303650	39578	79361
470	-22068.3996282	-22068.3996282	-22068.3968578	-22068.3982430	47527	85201
480	-23004.0145930	-23004.0229249	-23004.0141123	-23004.0173129	47047	91169
490	-23959.0165449	-23959.0165449	-23959.0143044	-23959.0128288	38993	92230
500	-24933.3757645	-24933.3757645	-24933.3757645	-24933.3757645	52075	98380
#Better	2		6		20	
#Equal	18		8		0	
#Worse	2		6		0	

keeping other components unchanged. Based on 20 representative instances with the logarithmic potential, we ran HEA and HEA* 5 times on each instance where each run was limited to 2×10^4 local optimizations. The experimental results are reported in Table 6 with the same information as in Table 5.

Table 6 shows that HEA and HEA* are comparable in terms of solution quality, but HEA is much faster than HEA* in terms of computational speed. Specifically, in terms of E_{best} , HEA obtains a better, equal and worse result

than HEA* respectively for 2, 18 and 2 instances. Looking at the average result E_{avg} , one can see that HEA gives a better, equal and worse result than HEA* for 6, 8 and 6 instances, respectively. In terms of computational time, HEA is about two times faster than HEA*. This experiment shows that the early-stopping strategy is able to significantly speed up the search without sacrificing the quality of solution.

6. Conclusions and Future Work

We presented in this study a population-based global optimization algorithm for the minimum energy configuration problems with the Coulombic and logarithmic potentials on the unit sphere, which have a number of applications in mathematics, physics, biology and chemistry. The algorithm is based on a general approach that transforms the initial constrained minimization problem into an unconstrained problem. Based on a population of high-quality solutions, the proposed algorithm explores new high-quality configurations by alternating a perturbation and a two-phase local optimization with an early-stopping strategy. The algorithm is reinforced by a population regeneration technique and a distance-based updating strategy. Computational results show that the algorithm performs remarkably well on the classic Thomson instances. In particular, the algorithm is able to improve the best-known solution of one instance of the classic Thomson problem ($N = 360$).

The configurations of N particles on a sphere are systematically optimized by the proposed algorithm for the classic discrete logarithmic potential. The structural evolution and characteristics of putative optimal configurations are analyzed for instances with $N \leq 500$ and several selected large instances. Computational results show that the logarithmic and Coulombic potentials have a high similarity on the ground-state configurations and that for the two potentials the best-known solutions have the same configuration for most sizes of $N \leq 400$.

The present work can be extended from several directions. First, the proposed algorithm is very general and can be applied to other minimum energy configuration problems on the surface of a sphere and other curved surface. Moreover, with a proper distance measure between the solutions, the proposed algorithm can be adapted to a number of global optimization problems involving N particles, such as the equal sphere packing problem and the structural optimization of atomic clusters. Second, it would be interesting to investigate new techniques (e.g., the block-coordinate descent method) to speed up the local optimization for large instances, since the time complexity of local optimization is very high and increases quadratically with the number of particles. Third, to handle large instances, decomposition methods and dimension reduction strategies can be integrated into the proposed algorithm. Fourth, the performance of the algorithm can be further enhanced by developing more efficient perturbation strategies and crossover operators for the optimization problems on the sphere. Finally, it would be interesting to apply the proposed algorithm to related applications discussed in the introduction and to evaluate the practical impact of this work.

Acknowledgments. We are grateful to the reviewers for their valuable comments and suggestions which helped us to improve the paper. We thank the Beijing Beilong Super Cloud Computing Co., Ltd (<http://www.blsc.cn/>) for providing HPC resources that have contributed to the computational experiments reported in this work. This work was partially supported by the National Natural Science Foundation of China (Grant Nos. 61703213 and 61933005).

References

- Addis, B., Locatelli, M., Schoen, F., 2008. Disk packing in a square: a new global optimization approach. *INFORMS Journal on Computing* 20, 516–524.
- Altschuler, E.L., Williams, T.J., Ratner, E.R., Tipton, R., Stong, R., Dowla, F., Wooten, F., 1997. Possible global minimum lattice configurations for Thomson's problem of charges on a sphere. *Physical Review Letters* 78, 2681.
- Baker, T., Olson, N., Fuller, S., 1999. Adding the third dimension to virus life cycles: three-dimensional reconstruction of icosahedral viruses from cryo-electron micrographs. *Microbiology and Molecular Biology Reviews* 63, 862–922.
- Bowick, M., Cacciuto, A., Nelson, D.R., Travesset, A., 2002. Crystalline order on a sphere and the generalized Thomson problem. *Physical Review Letters* 89, 185502.
- Calef, M., Griffiths, W., Schulz, A., 2015. Estimating the number of stable configurations for the generalized Thomson problem. *Journal of Statistical Physics* 160, 239–253.
- Calkin, M., Kiang, D., Tindall, D., 1986. Minimum energy configurations. *Nature* 319, 454–454.
- Dao, S.D., Abhary, K., Marian, R., 2017. An innovative framework for designing genetic algorithm structures. *Expert Systems with Applications* 90, 196–208.
- Doye, J.P., Leary, R.H., Locatelli, M., Schoen, F., 2004. Global optimization of Morse clusters by potential energy transformations. *INFORMS Journal on Computing* 16, 371–379.

- Doye, J.P., Miller, M.A., Wales, D.J., 1999. The double-funnel energy landscape of the 38-atom Lennard-Jones cluster. *The Journal of Chemical Physics* 110, 6896–6906.
- Dragnev, P.D., Legg, D.A., Townsend, D.W., 2002. Discrete logarithmic energy on the sphere. *Pacific Journal of Mathematics* 207, 345–358.
- Erber, T., Hockney, G., 1995. Comment on “Method of constrained global optimization”. *Physical Review Letters* 74, 1482.
- Grosso, A., Jamali, A., Locatelli, M., Schoen, F., 2010. Solving the problem of packing equal and unequal circles in a circular container. *Journal of Global Optimization* 47, 63–81.
- Grosso, A., Locatelli, M., Schoen, F., 2007. A population-based approach for hard global optimization problems based on dissimilarity measures. *Mathematical Programming* 110, 373–404.
- Grosso, A., Locatelli, M., Schoen, F., 2009. Solving molecular distance geometry problems by global optimization algorithms. *Computational Optimization and Applications* 43, 23–37.
- Gudla, P.K., Ganguli, R., 2005. An automated hybrid genetic-conjugate gradient algorithm for multimodal optimization problems. *Applied Mathematics and Computation* 167, 1457–1474.
- Hager, W.W., Zhang, H., 2005. A new conjugate gradient method with guaranteed descent and an efficient line search. *SIAM Journal on Optimization* 16, 170–192.
- Hager, W.W., Zhang, H., 2013. The limited memory conjugate gradient method. *SIAM Journal on Optimization* 23, 2150–2168.
- Hao, J.K., 2012. Memetic algorithms in discrete optimization, in: *Handbook of Memetic algorithms*. Springer, pp. 73–94.
- Hardin, D., Saff, E., 2005. Minimal Riesz energy point configurations for rectifiable d-dimensional manifolds. *Advances in Mathematics* 193, 174–204.
- Katanforoush, A., Shahshahani, M., 2003. Distributing points on the sphere, I. *Experimental Mathematics* 12, 199–209.
- Kroto, H.W., Heath, J.R., O’Brien, S.C., Curl, R.F., Smalley, R.E., 1985. C₆₀: Buckminsterfullerene. *Nature* 318, 162–163.
- Leary, R.H., 2000. Global optimization on funneling landscapes. *Journal of Global Optimization* 18, 367–383.
- Li, S., Roy, P., Travesset, A., Zandi, R., 2018. Why large icosahedral viruses need scaffolding proteins. *Proceedings of the National Academy of Sciences* 115, 10971–10976.
- Liu, D.C., Nocedal, J., 1989. On the limited memory BFGS method for large scale optimization. *Mathematical Programming* 45, 503–528.
- Lyakhov, A.O., Oganov, A.R., Stokes, H.T., Zhu, Q., 2013. New developments in evolutionary structure prediction algorithm USPEX. *Computer Physics Communications* 184, 1172–1182.
- Martín-Bravo, M., Llorente, J.M.G., Hernández-Rojas, J., Wales, D.J., 2021. Minimal design principles for icosahedral virus capsids. *ACS nano* 15, 14873–14884.
- McAllister, S.R., Floudas, C.A., 2010. An improved hybrid global optimization method for protein tertiary structure prediction. *Computational Optimization and Applications* 45, 377–413.
- Mehta, D., Chen, J., Chen, D.Z., Kusumaatmaja, H., Wales, D.J., 2016. Kinetic transition networks for the Thomson problem and Smale’s seventh problem. *Physical Review Letters* 117, 028301.
- Mehta, D., Chen, T., Morgan, J.W., Wales, D.J., 2015. Exploring the potential energy landscape of the Thomson problem via Newton homotopies. *The Journal of Chemical Physics* 142, 194113.
- Morris, J., Deaven, D., Ho, K., 1996. Genetic-algorithm energy minimization for point charges on a sphere. *Physical Review B* 53, R1740.
- Pérez-Garrido, A., Dodgson, M., Moore, M., Ortuno, M., Diaz-Sanchez, A., 1997. Comment on “possible global minimum lattice configurations for Thomson’s problem of charges on a sphere”. *Physical Review Letters* 79, 1417.
- Ridgway, W.J., Cheviakov, A.F., 2018. An iterative procedure for finding locally and globally optimal arrangements of particles on the unit sphere. *Computer Physics Communications* 233, 84–109.
- Saff, E.B., Kuijlaars, A.B., 1997. Distributing many points on a sphere. *The Mathematical Intelligencer* 19, 5–11.
- Shang, C., Zhang, D., Yang, Y., 2021. A gradient-based method for multilevel thresholding. *Expert Systems with Applications* 175, 114845.
- Shao, G., Shangguan, Y., Tao, J., Zheng, J., Liu, T., Wen, Y., 2018. An improved genetic algorithm for structural optimization of Au-Ag bimetallic nanoparticles. *Applied Soft Computing* 73, 39–49.
- She, B., Fournier, A., Yao, M., Wang, Y., Hu, G., 2022. A self-adaptive and gradient-based cuckoo search algorithm for global optimization. *Applied Soft Computing* 122, 108774.
- Smale, S., 1998. Mathematical problems for the next century. *The Mathematical Intelligencer* 20, 7–15.
- Thomson, J.J., 1904. On the structure of the atom: an investigation of the stability and periods of oscillation of a number of corpuscles arranged at equal intervals around the circumference of a circle; with application of the results to the theory of atomic structure. *The London, Edinburgh, and Dublin Philosophical Magazine and Journal of Science* 7, 237–265.
- Vitela, J.E., Castaños, O., 2012. A sequential niching memetic algorithm for continuous multimodal function optimization. *Applied Mathematics and Computation* 218, 8242–8259.
- Wales, D.J., 2022. The cambridge energy landscape database. Figshare <http://www-wales.ch.cam.ac.uk/CCD.html>.
- Wales, D.J., Doye, J.P., 1997. Global optimization by basin-hopping and the lowest energy structures of Lennard-Jones clusters containing up to 110 atoms. *The Journal of Physical Chemistry A* 101, 5111–5116.
- Wales, D.J., McKay, H., Altschuler, E.L., 2009. Defect motifs for spherical topologies. *Physical Review B* 79, 224115.
- Wales, D.J., Scheraga, H.A., 1999. Global optimization of clusters, crystals, and biomolecules. *Science* 285, 1368–1372.
- Wales, D.J., Ulker, S., 2006. Structure and dynamics of spherical crystals characterized for the Thomson problem. *Physical Review B* 74, 212101.
- Wei, G.W., 2019. Protein structure prediction beyond AlphaFold. *Nature Machine Intelligence* 1, 336–337.
- Wille, L., 1986. Searching potential energy surfaces by simulated annealing. *Nature* 324, 46–48.
- Zandi, R., Dragnea, B., Travesset, A., Podgornik, R., 2020. On virus growth and form. *Physics Reports* 847, 1–102.
- Zhou, Q., Hao, J.K., Wu, Q., 2021. Responsive threshold search based memetic algorithm for balanced minimum sum-of-squares clustering. *Information Sciences* 569, 184–204.